Climate variability and density-dependent population dynamics: Lessons from a simple High-Arctic ecosystem

Running title: Climate and density-dependent dynamics

Dominique Fauteux[1], Audun Stien[2], Nigel G. Yoccoz[2], Eva Fuglei[3], and Rolf A. Ims[2]

[1]Canadian Museum of Nature, Centre for Northern Studies, Gatineau (QC) Canada.
[2]Department of Arctic and Marine Biology, UiT The Arctic University of Norway, Tromsø, Norway.
[3]Norwegian Polar Institute, Tromsø, Norway

Statement of authorship
DF wrote the first complete draft of the manuscript and conducted CMR analyses; AS collected data in the field, conducted population modelling, and contributed substantially to revisions; NGY, EF and RAI collected data and contributed substantially to revisions.

Corresponding author:
Dominique Fauteux
1740, chemin Pink
Gatineau (QC) J9H 6Y8
Canada

Contact (e-mail) and competing interest information
Dominique Fauteux (corresponding author) : dfauteux@nature.ca
Audun Stien : audun.stien@uit.no
Nigel G. Yoccoz : nigel.yoccoz@uit.no
Eva Fuglei : eva.fuglei@npolar.no
Rolf Ims: rolf.ims@uit.no
All authors have no competing interest to declare.

Data accessibility
All data used in this work will be deposited in a public repository (i.e. Dryad) upon request or publication.

Abstract
Ecologists are still puzzled by the diverse population dynamics of herbivorous small mammals that range from high-amplitude, multi-annual cycles to stable dynamics. Theory predicts that this diversity results from combinations of climatic seasonality, weather stochasticity and density-dependent food web interactions. The almost ubiquitous 3-5-yr cycles in boreal and arctic climates may theoretically result from bottom-up (plant-herbivore) and top-down (predator-prey) interactions. Assessing empirically the roles of such interactions, and how they are influenced by environmental stochasticity, has been hampered by food web complexity. Here, we take advantage of a uniquely simple High-Arctic food web, which allowed us to analyze dynamics of a

46 graminivorous vole population not subjected to top-down regulation. This population
47 exhibited high-amplitude, non-cyclic fluctuations - partly driven by weather stochasticity.
48 However, the predominant driver of the dynamics was direct density dependence, which
49 alternated between being weak in summer and strong (overcompensatory) in winter that
50 the population frequently crashed. Model simulations showed that this season-specific
51 density dependence would yield regular 2-year cycles in absence of stochasticity. While
52 such short cycles have not yet been observed in mammals, they are theoretically plausible
53 if graminivorous vole populations are deterministically bottom-up regulated. When
54 incorporating weather stochasticity in the model simulations, cyclicity became disrupted
55 and the amplitude was increased - akin to the observed dynamics. Our findings contrast
56 with the 3-5-yr population cycles involving delayed density dependence that are typical
57 of graminivorous small mammals in more complex food webs, suggesting that top-down
58 regulation is an important component of such dynamics.

59
60 **Keywords:** population fluctuations; tundra ecosystem; trophic interactions; seasonality;
61 top-down regulation; climate change.
62

63 **Significance** (max 120 words)

64 Whether the renowned population cycles of small mammals in northern food webs are
65 driven by bottom-up (plant-herbivore) or top-down (predator-prey) interactions is still a
66 debated question, but crucial to our understanding of their ecological functions and
67 response to climate change. A long-term study of a graminivorous vole population in an
68 exceptionally simple High-Arctic food web, allowed us to identify which population
69 dynamics features are present when top-down regulation is absent. Unique features were
70 high-amplitude, non-cyclic population fluctuations driven by a combination of stochastic
71 weather events and season-specific direct density dependence likely arising from plant-
72 herbivore interactions. That such features are not present in more complex food webs,
73 points to the importance of top-down regulation in most small mammal populations.

74
75 **Introduction**
76 Theory suggests that contrasting population dynamics result from details in the pattern of
77 density dependence, including its strength, whether it acts instantly or with a delay, and
78 how it interacts with deterministic (seasonal) and stochastic (weather) components of the
79 prevailing or changing climate (1-5). Studies of small rodents have contributed much to
80 elucidating the different facets of density-dependent and density-independent population
81 dynamics (2, 4). A central topic has been what sort of density dependence yields the
82 high-amplitude, multi-annual population cycles - for which voles and lemmings have
83 become so renowned (6-9). Based on time series analyses, delayed density dependence is
84 considered to be a main determinant of population cycles (see (4, 10) for reviews),
85 although overcompensatory direct density dependence appears to be an alternative in
86 some settings (11). As rodent cycles are most prevalent in northern ecosystems with
87 profound climatic seasonality (6, 7, 12, but see 13, 14), several studies have emphasised

88   that annual density dependence ought to be decomposed into its seasonal components
89   (15-17) - both to accurately account for the density-dependent structure that underlies the
90   observed dynamics and to identify the season-specific biotic mechanisms that cause
91   density dependence. Considering seasonal dynamics is also crucial to assessing the role
92   of climatic change and weather stochasticity, because both differ between summer and
93   winter (15, 18). The role of climate forcing is now also emphasized by the recent
94   collapses and dampening of population cycles in several ecosystems that appear to be
95   associated with ongoing climate change (15, 19, 20).
96   Linking density dependence to the biotic mechanisms that causally generate the
97   diversity of population dynamic patterns seen in small mammals, has proved to be
98   challenging. Most rodent populations are imbedded in complex food webs, and hence,
99   simultaneously subjected to a multitude of biotic interactions that could cause the
100 different facets of density-dependent population growth. For instance, delayed and direct
101 density dependence may result from both top-down and bottom-up trophic interactions as
102 well as intrinsic population mechanisms (11, 21, 22). While field experiments have
103 helped pinpointing some mechanisms (23-27), they have been too short-term to be
104 conclusive with respect to what generates different patterns of multi-annual population
105 dynamics.
106   Here we apply an approach that has proved useful for unravelling the effects of
107 density dependence and weather stochasticity in herbivorous large mammals (e.g. 28-30),
108 namely to target populations that are found in exceptionally simple biotic settings. Hence,
109 our study targets a High-Arctic population of the graminivorous (grass-eating) East
110 European vole (*Microtus levis*) in a food web that lacks significant top-down regulation
111 (i.e. predation). By combining statistical analyses of long-term, high-quality live-trapping
112 data with simulations of a population model parameterized from these data, we (1)
113 identify which features of density dependence (e.g. direct or delayed) and resultant
114 population dynamics (e.g. cyclic or non-cyclic) that emerge in such a simple biotic
115 setting, and (2) assess how climatic seasonality and weather stochasticity impinge on
116 such density-dependent population dynamics. Finally, we point out how the insights from
117 this unique case study shed new light on the longstanding puzzle about what generates
118 population cycles and how ongoing climate change may influence these cycles.
119
120 **Methods**
121 *Study population*
122 Our study was located at Grumant in Svalbard (78.18°N, 15.13°E). This High-Arctic
123 location is characterised by cool summers (July average: 5.9°C) and cold winters
124 (January average -16.2°C) with little precipitation (average 190 mm, period 1960-1990;
125 31). Average daily air temperatures are typically above 0°C from early-to-mid June –
126 September (data from Longyearbyen airport, ~13 km away from Grumant). Winter
127 temperatures are much more variable than summer temperatures (31, 32). Rain-on-snow
128 (ROS) are relatively frequent stochastically occurring weather events (30) and have been
129 found to strongly influence the population dynamics of all year-round resident vertebrate
130 populations in Svalbard (33).
131   The East European vole belongs to one of the most speciose and widespread
132 genera (*Microtus*) of small mammals (34). Most *Microtus* species are graminivorous
133 (grass-eating) and have multivoltine life histories (e.g. multiple generation per year). The

134 East European vole was accidentally introduced to Svalbard in the first half of the 20th
135 century (35). The voles have a highly restricted distribution on the archipelago,
136 associated with seabird fertilized tundra vegetation dominated by graminoids (36).
137   There are no other small mammals present in Svalbard, which suggests no
138 interspecific competition (37). The Arctic fox (*Vulpes lagopus*) is the only terrestrial
139 predator present, but acts as a generalist carnivore that mostly relies on large colonies of
140 seabirds in the study area (38). Thus, the focal food web lacks the guild of specialist
141 predators consisting of mustelids, owls, hawks and jaegers that are almost omnipresent in
142 the Arctic (12). East European voles reproduce quickly with females observed to be
143 gravid as early as 17 days old (39) and may live at high population densities (>100 ind.
144 ha^{-1}; 37). Many *Microtus* populations have been studied extensively on the European
145 continent where they typically exhibit 3-5-yr multi-annual cycles (11, 13-15).
146
147 *Live trapping*
148 East European voles were live-trapped during the years 1990-2007. Here, we analysed
149 two data sets. The main data set used for analysis of seasonal density dependence and
150 demography was obtained from one of the largest and lushest vole habitat patches in
151 Svalbard; hereafter termed Core area (Fig. 1). From 1990 to 1996, we used a trapping
152 grid of 93 Ugglan Special multiple-capture traps encompassing 4.5 ha of the Core area,
153 while from 2002-2006 the grid was made of 74 traps and encompassed 2.8 ha. Traps
154 were separated by approximately 20 m and placed by burrow entrances wherever
155 possible. Trapping of the Core area followed the robust design of Pollock (40) and
156 consisted of three primary periods (late June/early July [hereafter termed July] = P1;
157 early August = P2; and early September = P3), each with 6 to 10 secondary periods,
158 except in 1990 when primary periods spanned only the first half of the summer. The
159 primary trapping periods consisted of traps being checked at 13h00 and 19h00 after
160 bating with oats and potatoes in the morning (07h00, i.e. 2 secondary periods per day).
161 Traps were deactivated during the last trapping period of the day. We used a second,
162 more long-term data set obtained from a linear habitat on a ridge and vegetated part of the
163 ravine at the western edge of the Core area (hereafter termed Ridge; Fig. 1) for assessing
164 the annual population dynamics. The Ridge area was monitored with 30 traps in August
165 during 1991-2007, with the same number of secondary periods as for the Core area.
166 Captured voles were marked by toe clipping, sexed and weighed. The study was
167 conducted according to the regulations for research in Svalbard during the study period.
168
169 *Density estimation*
170 The densities of the vole population in the Core and Ridge areas were estimated by
171 spatially-explicit capture-recapture (SECR) models with the package *secr* in R (41-43).
172 Briefly, these models have the advantage of estimating capture probabilities based on the
173 distance separating the center of activities of an individual from a trap (43). By using a
174 two-parameter half-normal detection function, we obtained more accurate estimates of
175 the area effectively surveyed (44). For the Core area, we used one null SECR model per
176 trapping period per year with the Huggins parameterisation to estimate density (44). For
177 the Ridge area, annual densities were obtained for the August trapping period only.
178 Densities of male and female adults (body mass ≥25 g) and sub-adults (body mass <25 g;
179 39) were derived from this general model. Because the movement of voles in Svalbard is

180   restricted by habitat, we used a 20 m buffer around traps to build the state-space that is
181   used to estimate effective sampling area. The Nelder-Mead algorithm was used for
182   optimisation of the likelihood in model fitting.
183
184   *Annual density-dependent structure and temporal variability*
185   We used the annual early August SECR density estimates from the Ridge area to assess
186   the density-dependent structure of the population dynamics. We modelled ln-transformed
187   densities from the 18-year time series using a second-order autoregressive model (2, 4).
188   Coefficients obtained from this type of model inform about direct (β_{t-1}) and delayed
189   density dependence (β_{t-2}), and may also be interpreted with respect to the presence of
190   cyclic dynamics and cycle periods (1). We observed zero vole densities in the Ridge area
191   in 1996 and 2002 and the time series was modelled using $\log(D_t + c)$ with $c = 1$. A range
192   of values for c, from $c = 0.2$ to $c = 2$, were investigated, but the choice of c was not found
193   to affect parameter estimates and conclusions substantially. We used the standard
194   deviation of the log10 transformed time series as a metric for the temporal variability (i.e.
195   the amplitude) of the multiannual dynamics (s-index; 45). The s-index has been used both
196   to define cyclic dynamics (index values > 0.5; 46) and to compare populations across
197   environmental gradients (47-49).
198
199   *Seasonal density dependence and climate effects on population growth*
200   We used the following model to explore patterns of variation in population growth in
201   summer and winter in the Core area:
202
203   $$X_{t+1} = X_t * e^{r_t * \Delta t} \hspace{3cm} (1)$$
204
205   Where X_t is the true population density at time t, r_t is the population growth rate from t to
206   t+1 and Δt is the time period from t to $t+1$ (in months). Furthermore, we modelled r_t as a
207   linear function of X_t, weather stochasticity in winter (C_t, i.e. ROS) and residual stochastic
208   variation in r (process error, ε_t):
209
210   $$r_t = \beta_0 + \beta_X * X_t + \beta_C * C_t + \varepsilon_t \hspace{2cm} (2)$$
211
212   where we assume that process error $\varepsilon_t \sim N(0, \sigma_r^2)$ and β_0, β_X, β_C and σ_r^2 are parameters
213   estimated by the data. Measurement error was included in the model assuming a log
214   normal distribution for the densities estimated using the SERC model, D_t, giving:
215
216   $$D_t \sim \text{lnorm}(\log_e(X_t), \sigma_{D,t}^2) \hspace{2.5cm} (3)$$
217
218   The log normal measurement error standard deviations, $\sigma_{D,t}$, were calculated from the
219   estimates of the standard error of D_t (SE(D_t)) obtained in the SECR analysis:
220
221   $$\sigma_{D,t} = \log_e((\text{SE}(D_t) / D_t)^2 + 1) \hspace{2cm} (4)$$
222
223   The model (equations 1-3) was fitted in JAGS version 4.2.0 (50). Point estimates
224   of r_t and associated 95 % credibility intervals presented in figures were obtained by
225   fitting a model for r_t (equation 2) with time fitted as a factor, i.e. $r_t = \beta_t$. In addition to

226   parameter estimates and associated 95% credibility intervals we report estimates of
227   Bayesian R^2 for the models (51). The Bayesian R^2 was calculated as the mean of $R_i^2 =$
228     $\text{var}(\text{fit}_i) / (\text{var}(\text{fit}_i) + \text{var}(\text{residuals}_i))$, where i is the index of draws in MCMC chains,
229     $\text{var}(\text{fit}_i) = \text{var}(\beta_{0,i} + \beta_{X,i} * X_t + \beta_{C,i} * C_t)$ and $\text{var}(\text{residuals}_i) = \sigma_{r,i}^2$.

230   Analyses of population growth were done separately for the approximately 2.5
231   month summer period (June/July-September) and for the approximately 9.5 month winter
232   period (September-June/July) as we expected the population dynamics to differ
233   substantially in these two seasons. In the winter we expected the amount of ROS to affect
234   population growth (33, 52).

235   Summer population growth could be estimated from the change in densities from
236   June/July (t) to August ($t + 1$) and from August ($t + 1$) to September ($t + 2$). Differences
237   between these periods were investigated by fitting period as a factor in the model for
238   population growth (equation 2). Population growth rates were not estimated for the
239   summer of 1996, when there were no voles captured in the study area, and 2002, when
240   there were no voles captured in the first and second primary trapping periods and an
241   estimate of 1 vole per hectare (3 voles caught) in the third primary period. The very low
242   density estimates in September 2002 and the absence of voles in 1996 implied adoption
243   of methodological adjustments, that are detailed in supplementary material, to allow
244   growth rate estimates over the associated winters.

245   The timing of the primary trapping periods differed somewhat in 1990-1991 from
246   subsequent years. In 1990, all the trapping was early in the season and the time period
247   from primary period 1 to primary period 3 was only 0.7 months. We therefore only used
248   data from primary period 1 and 3 to estimate population growth, to get a time period that
249   was more similar to the other years ($\Delta t = 1.2$-1.7 months). In 1991 it was only 2 weeks
250   between primary period 1 and 2 and we used only estimates from primary period 2 and 3
251   in analyses.

252

253   *Model simulations of multiannual population dynamics*
254   We simulated the annual population dynamics linking summer and winter population
255   growth using:

256

257         $X_{a,t+1} = X_{s,t} * e^{r_{s,t} * \Delta t_s}$ (5)
258         $X_{s,t+1} = X_{a,t} * e^{r_{w,t} * \Delta t_w}$ (6)

259

260   where $X_{s,t}$ and $X_{a,t}$ is population density in the spring and autumn in year t respectively,
261     $r_{s,t}$ and $r_{w,t}$ are population growth rates (month^{-1}) in summer and winter respectively, and
262   Δt_s and Δt_w are the time periods of the summer and winter seasons respectively ($\Delta t_s +$
263     $\Delta t_w = 12$).

264   Using equation (2), $r_{j,t}$ were modelled with parameters estimated from the data
265   (Table 2). Our baseline deterministic model included only density dependence ($r_{j,t} = \beta_{j,0} +$
266     $\beta_{j,X} * X_{j,t}$) and assumed 3 months of summer and 9 months of winter. The sensitivity of
267   population dynamics to changes in parameter values were evaluated using bifurcation
268   diagrams and analyses of autocorrelation.

269

270   *Demography*

271   The demographic structure of the population was analysed using SECR based estimates
272   of subadult and adult, male and female vole densities. Recruitment was determined by
273   comparing densities of subadults to adult female densities. We analysed densities of male
274   and female voles within age categories to detect sex differences.
275   Survival and maturation rates of subadult and adult, male and female voles were
276   estimated using multi-event models implemented in the software E-Surge (53). The
277   summer estimates were obtained for the periods of July-August and August-September.
278   The data did not allow demographic rates to be estimated for the winter period
279   (September-July), because too few individuals captured in year t survived the winter and
280   were recaptured year $t+1$. The maturation rate is the probability of a subadult to develop
281   into the adult stage from one primary period to the next. Survival, maturation and
282   detection probabilities were modelled as functions of covariates using a logit link
283   function. Year, period (July-August vs. August-September) and sex were considered as
284   covariates for all demographic rates. In addition, age (subadults vs. adults) was
285   considered in models for survival and detection rates. Furthermore, we evaluated the
286   effect of vole density, D_t, as an environmental covariate in models of survival and
287   maturation rates. Model selection was based on Akaike information criterion corrected
288   for overdispersion (QAICc; 54) and estimates used in the simulations (see below) were
289   retained from the model judged as the most parsimonious using QAICc.
290   The effect of density on survival and maturation was first determined by whether
291   the covariate was significant in the most parsimonious, non-temporal model. If yes, we
292   tested if the variance explained by the covariate was significant using ANODEV with M_t
293   being a model with year fitted as a factor, M_c being a model with D_t fitted as a continuous
294   covariate, and M_0 being the model without density or time included as covariates (55).
295
296   **Results**
297   *Annual population dynamics*
298   The 1991-2007 time series of Eastern European vole densities from the Ridge trapping
299   area was characterised by high amplitude population fluctuations with 2 - 4 years
300   between subsequent crash years (Fig. 1). The population dynamics appeared to be
301   stationary; i.e. there was no evidence for temporal trends in mean or variance in densities
302   over the 18 years. The amplitude of the fluctuations (s-index=0.57) was within the range
303   found in population time series of cyclic Arctic lemming populations (49). However, in
304   contrast to most other Arctic populations, first (r = -0.39) and second-order (r = 0.02)
305   autocorrelation coefficients showed no evidence of cyclic dynamics. A second-order
306   autoregressive model supported direct density dependence (β_{t-1} = -0.46, 95% confidence
307   interval [CI]: [-0.70, 0.02]), while delayed density dependence was estimated to be close
308   to zero (β_{t-2}= -0.15, 95% CI: [-0.65, 0.34]). These estimates suggest population dynamics
309   with dampened 2-year cycles (1), and that sustained fluctuations were upheld by high
310   unstructured error variance (σ^2 = 1.3).
311
312   *Seasonal density dependence*
313   Population densities in the Core trapping area showed the same annual pattern as
314   densities in the Ridge area (cross-correlation of vole densities with the Ridge trapping
315   area, r = 0.92; Fig. 1). Within the summer season, population growth rates were all
316   positive (Fig. 2 and 3a). This suggests that vole population densities remained below

317 carrying capacity in summer. Still, there was evidence for weak negative density
318 dependence in the population growth rates (Table 1, Fig. 3a).
319   In contrast, winter population growth rates were negative in many of the years.
320 The negative population growth rates in winter were associated with both high vole
321 densities in the previous autumn and high levels of ROS in the winter (Table 1, Fig. 3b).
322 Overall, the data suggest strong population regulation from direct density dependence in
323 the winter period.
324
325 *Simulated population dynamics*
326 Simulation of the deterministic version of the seasonal density-dependent model (eq. 2, 5-
327 6) generated stable 2-year vole cycles. These 2-yr cycles were relatively robust to
328 changes in climate severity in winter, in that high ROS must become the norm before we
329 expect a change to stable dynamics with a single equilibrium density (Fig. 4a). The 2-yr
330 cycle in the baseline model was also robust to changes in season lengths as climate
331 change would have to reduce the winter length to well below 8 months for more complex
332 dynamics to appear (Fig. 4b). However, the signal of the 2-yr cycles deteriorated rapidly
333 with increasing levels of stochastic process error (Fig. 4c). At the observed levels of
334 process error, as generated by stochastic variation in winter ROS, the expected second
335 order autocorrelation was close to zero in the model simulations (r = 0.02); i.e. similar to
336 what was estimated from the time series data. Finally, temporal variability as quantified
337 by the s-index increased with increasing process error (Fig. 4d).
338
339 *Demography*
340 Sub-adult male and female voles occurred at similar densities, with no evidence for a
341 systematic deviance from a 1:1 sex ratio (Fig. 5a). In contrast, the sex ratio of adults
342 approached a female-bias of 2:1 at high female densities (Fig. 5b). This pattern was
343 consistent with strong density-dependent regulation of adult male densities in summer,
344 with growth rates close to zero at ~14 adult male voles ha^{-1} (Fig. 5c). There was no strong
345 evidence for adult female population growth to be density-dependent in summer (β_D = -
346 0.015, CI=[-0.034, 0.005]). Recruitment in the population remained also relatively stable
347 across densities (Fig. 5d).
348   Both survival and maturation rates varied significantly between years as well as
349 among demographic categories (sex and age) and summer periods (Supplementary
350 material, Table S1, Fig. S1) in a manner that contributed to the high process error in
351 summer population growth (Table 1). Survival rates were density-dependent, and
352 stronger in females than in males (Supplementary material, Table S2, Fig. S2), whereas
353 there was no evidence for density dependence in maturation rates (Supplementary
354 material, Table S2, Fig. S3).
355
356 **Discussion**

357 Without significant top-down regulation from predators or interspecific competition, the
358 focal study system is essentially reduced to a simple two-link food chain consisting of a
359 multivoltine herbivore population and their graminoid food plants in a profoundly
360 seasonal environment. Here we have presented the first empirical analysis of such an
361 ecological system that previously has been subjected to only theoretical investigations.

362 Such systems have been modelled mechanistically in continuous time to identify under
363 which circumstances multiannual herbivore population cycles can be expected (56, 57).
364 Moreover, theoreticians have thoroughly investigated the dynamical properties of
365 phenomenological discrete-time models with seasonal direct density dependence (58),
366 akin to the model we parameterized here with field data. The core insight from this theory
367 - and indeed also our empirical study - is that the profound seasonality destabilises the
368 dynamics of such simple systems (59). Profound seasonality in terms of a long Arctic
369 winter without primary production implies that the carrying capacity in summer greatly
370 exceeds that of the winter. Such environmental setting combined with a multivoltine life
371 history and rapid population growth in summer allows the herbivore population to
372 overshoot its winter carrying capacity. We provide evidence that such situation prevails
373 in the graminivorous East European voles on Svalbard. Here season-specific, direct
374 density-dependent growth alternated between being weak in summer and so strong
375 (overcompensatory) in winter that the population crashed whenever having attained high
376 densities at the end of the summer.
377   Interestingly, the continuous-time, plant-herbivore model analysed by Turchin
378 and Batzli (57) with a graminoid-type plant regrowth function, multivoltine herbivore
379 population dynamics and High-Arctic seasonality without stochasticity, generated 2-year
380 cycles similar to our baseline model. However, we are not aware of such short population
381 cycles have ever been reported for any mammal population. Neither are we aware of any
382 other examples of the non-cyclic high-amplitude, high frequency boom-bust vole
383 population dynamics we observed in our High-Arctic study system. In multivoltine
384 rodents, cycle lengths typically vary between 3-5 years in ecosystems with profound
385 seasonality, while populations in environments with less pronounced seasonality have
386 typically non-cyclic low-amplitude fluctuations that often are categorised as stable
387 dynamics (48, 60). It is commonly assumed that cycle generating mechanisms induce
388 delayed density dependence (4, 10, 12, 21), while opinions differ about which
389 mechanisms are in place (61, 62). Seasonality is in itself a source of delay in producer-
390 consumer interactions (56), but is expected to yield at most 2-year cycles. Also, the rapid
391 regrowth of graminoids (57) – even after high vole peak densities and severe winter
392 grazing (63) – prevents longer delays that may generate the longer cycles often found in
393 graminivorous voles. We notice that the lack of evidence for delayed density dependence
394 in our study system may suggest that delays due to intrinsic mechanisms, such as stress-
395 induced maternal effects (64), were of little importance. In fact, the only demographic
396 feature that could be attributed to intrinsic regulation was the adult sex ratio, which
397 became more female biased with increasing population density - as could be expected
398 from the polygynous mating system of graminivorous voles (65). Finally, our study is
399 consistent with the hypothesis that the almost ubiquitous guild of specialist rodent
400 predators in boreal and Arctic food webs normally cause delayed density dependence, in
401 that both the predator guild and delayed density dependence were lacking in our study
402 system (62, 66, 67). Indeed, the unique absence of top-down regulation by specialist
403 predators in High-Arctic Svalbard is the most likely cause of the exceptional vole
404 population dynamics observed. Experimental predator removals (24, 27, 63) have never
405 been conducted at sufficient spatial and temporal scale to investigate whether a similar
406 outcome would appear in other vole populations released from top-down regulation.

A fundamental question in population ecology accentuated by global climate change is how abiotic environmental variation can modify the effect of density-dependent biotic interactions. Our study adds to previous studies showing that episodes of mild winter weather in boreal and Arctic ecosystems may lead to population crashes in herbivores (68-70) and disrupt population cycles (18-20, 71). Previous models have shown that climatically disrupted population cycles in multivoltine rodents readily collapses to low-amplitude fluctuations and hence stable population dynamics in the presence of direct and delayed density dependence (19, 20, 71). Here we have shown that population cycles in a simple trophic system with only direct density dependence, may also be disrupted by increasing weather stochasticity, however, without any dampening effect on the dynamics. Hence, our case study provides support to the general conjecture that the impact of climate change on ecological systems depends on their structure and hence can be expected to be diverse across time and space (18, 19, 29).

References

1. T. Royama, *Analytical population dynamics*. Springer, Ed. (Chapman and Hall., 1992), pp. 371.
2. P. Turchin, *Complex population dynamics* (Princeton University Press, Princeton, New Jersey, 2003), pp. 451.
3. R. M. May, *Stability and complexity in model ecosystems* (Printeton University Press, Princeton, New Jersey, 2001).
4. N. C. Stenseth, Population cycles in voles and lemmings: density dependence and phase dependence in a stochastic world. *Oikos* **87**, 427-461 (1999).
5. O. N. Bjørnstad, B. T. Grenfell, Noisy clockwork: time series analysis of population fluctuations in animals. *Science* **293**, 638-643 (2001).
6. C. J. Krebs, *Population fluctuations in rodents* (The University of Chicago Press, Chicago, 2013).
7. C. S. Elton, *Voles, mice and lemmings. Problems in population dynamics.* (Clarendon press, Oxford, 1942), pp. 496.
8. J. P. Finnerty, *The population ecology of cycles in small mammals* (Yale University Press, New Haven, 1981), pp. 234.
9. N. C. Stenseth, R. A. Ims, *The biology of lemmings* (Academic press, London, 1993), pp. 683.
10. F. Barraquand *et al.*, Moving forward in circles: challenges and opportunities in modelling population cycles. *Ecol. Lett.* **20**, 1074-1092 (2017).

452 11. F. Barraquand, A. Pinot, N. G. Yoccoz, V. Bretagnolle, Overcompensation and phase
453   effects in a cyclic common vole population: between first and second-order cycles. *J.*
454   *Anim. Ecol.* **83**, 1367-1378 (2014).
455 12. R. A. Ims, E. Fuglei, Trophic interaction cycles in tundra ecosystems and the impact
456   of climate change. *Bioscience* **55**, 311-322 (2005).
457 13. E. Korpimaki *et al.*, Vole cycles and predation in temperate and boreal zones of
458   Europe. *J. Anim. Ecol.* **74**, 1150-1159 (2005).
459 14. X. Lambin, V. Bretagnolle, N. G. Yoccoz, Vole population cycles in northern and
460   southern Europe: Is there a need for different explanations for single pattern? *J.*
461   *Anim. Ecol.* **75**, 340-349 (2006).
462 15. T. Cornulier *et al.*, Europe-wide dampening of population cycles in keystone
463   herbivores. *Science* **340**, 63-66 (2013).
464 16. N. C. Stenseth *et al.*, Seasonality, density dependence, and population cycles in
465   Hokkaido voles. *Proc. Natl. Acad. Sci. U.S.A.* **100**, 11478-11483 (2003).
466 17. T. F. Hansen, N. C. Stenseth, H. Henttonen, Multiannual vole cycles and population
467   regulation during long winters: an analysis of seasonal density dependence. *Am. Nat.*
468   **154**, 129-139 (1999).
469 18. K. Korpela *et al.*, Nonlinear effects of climate on boreal rodent dynamics: mild
470   winters do not negate high-amplitude cycles. *Glob. Change Biol.* **19**, 697-710 (2013).
471 19. O. Gilg, B. Sittler, I. Hanski, Climate change and cyclic predator–prey population
472   dynamics in the high Arctic. *Glob. Change Biol.* **15**, 2634-2652 (2009).
473 20. R. A. Ims, J. A. Henden, S. T. Killengreen, Collapsing population cycles. *Trends*
474   *Ecol. Evol.* **23**, 79-86 (2008).
475 21. J. H. Myers, Population cycles: generalities, exceptions and remaining mysteries.
476   *Proc. R. Soc. B-Biol. Sci.* **285**, 20172841 (2018).
477 22. T. F. Hansen, N. C. Stenseth, H. Henttonen, J. Tast, Interspecific and intraspecific
478   competition as causes of direct and delayed density dependence in a fluctuating vole
479   population. *Proc. Natl. Acad. Sci. U.S.A.* **96**, 986-991 (1999).
480 23. R. S. Ostffeld, C. D. Canham, S. R. Pugh, Intrinsic density-dependent regulation of
481   vole populations. *Nature* **366**, 259-261 (1993).
482 24. R. A. Ims, H. P. Andreassen, Spatial synchronization of vole population dynamics by
483   predatory birds. *Nature* **408**, 194-196 (2000).
484 25. I. M. Graham, X. Lambin, The impact of weasel predation on cyclic field-vole
485   survival: the specialist predator hypothesis contradicted. *J. Anim. Ecol.* **71**, 946-956
486   (2002).
487 26. O. Huitu, M. Koivula, E. Korpimaki, T. Klemola, K. Norrdahl, Winter food supply
488   limits growth of northern vole populations in the absence of predation. *Ecology* **84**,
489   2108-2118 (2003).
490 27. D. Fauteux, G. Gauthier, D. Berteaux, Top-down limitation of lemmings revealed by
491   experimental reduction of predators. *Ecology* **97**, 3231-3241 (2016).
492 28. B. T. Grenfell *et al.*, Noise and determinism in synchronized sheep dynamics. *Nature*
493   **394**, 674-677 (1998).
494 29. T. Coulson *et al.*, Age, sex, density, winter weather, and population crashes in Soay
495   sheep. *Science* **292**, 1528-1531 (2001).
496 30. B. B. Hansen *et al.*, More frequent extreme climate events stabilize reindeer
497   population dynamics. *Nat. Commun.* **10**, 1616 (2019).

498   31. E. J. Førland, I. Hanssen-Bauer, P. Ø. Nordli, *Climate statistics and longterm series*
499   *of temperature and precipitation at Svalbard and Jan Mayen* (Norwegian
500   Meteorological Institute, Oslo, 1997).
501   32. N. G. Yoccoz, R. A. Ims, Demography of small mammals in cold regions: the
502   importance of environmental variability. *Ecol. Bull.* **47**, 137-144 (1999).
503   33. B. B. Hansen *et al.*, Climate events synchronize the dynamics of a resident vertebrate
504   community in the High Arctic. *Science* **339**, 313-315 (2013).
505   34. R. H. Tamarin, *Biology of new world Microtus* (American Society of Mammalogists,
506   United-States, 1985), pp. 893.
507   35. K. Fredga, M. Jaarola, R. Anker Ims, H. Steen, N. G. Yoccoz, The 'common vole' in
508   Svalbard identified as Microtus epiroticus by chromosome analysis. *Polar Res.* **8**,
509   283-290 (1990).
510   36. A. Elvebakk, A survey of plant associations and alliances from Svalbard. *J. Veg. Sci.*
511   **5**, 791-802 (1994).
512   37. E. Koivisto, O. Huitu, E. Korpimaki, Smaller *Microtus* vole species competitively
513   superior in the absence of predators. *Oikos* **116**, 156-162 (2007).
514   38. K. Frafjord, Predation on an introduced vole *Microtus rossiaemeridionalis* by arctic
515   fox *Alopex lagopus* on Svalbard. *Wildl. Biol.* **8**, 41-47 (2002).
516   39. N. G. Yoccoz, R. A. Ims, H. Steen, Growth and reproduction in island and mainland
517   populations of the vole Microtus epiroticus. *Can. J. Zool.* **71**, 2518-2527 (1993).
518   40. K. H. Pollock, A capture-recapture design robust to unequal probability of capture. *J.*
519   *Wildl. Manag.* **46**, 752-757 (1982).
520   41. M. G. Efford (2015) secr: spatially explicit capture-recapture models. R package
521   version 2.9.4. http://CRAN.R-project.org/package=secr.
522   42. R Core Team (2016) R: A language and environment for statistical computing. R
523   Foundation for Statistical Computing, Vienna, Austria.
524   43. D. L. Borchers, M. G. Efford, Spatially explicit maximum likelihood methods for
525   capture–recapture studies. *Biometrics* **64**, 377-385 (2008).
526   44. C. J. Krebs *et al.*, Density estimation for small mammals from livetrapping grids:
527   rodents in northern Canada. *J. Mammal.* **92**, 974-981 (2011).
528   45. N. C. Stenseth, E. Framstad, Reproductive Effort and Optimal Reproductive Rates in
529   Small Rodents. *Oikos* **34**, 23-34 (1980).
530   46. H. Henttonen, A. D. McGuire, L. Hansson, Comparisons of amplitudes and
531   frequencies (spectral analyses) of density variations in long-term data sets of
532   *Clethrionomys* species. *Ann. Zool. Fenn.* **22**, 221-227 (1985).
533   47. L. Hansson, H. Henttonen, Gradients in density variations of small rodents: the
534   importance of latitude and snow cover. *Oecologia* **67**, 394-402 (1985).
535   48. L. Hansson, H. Henttonen, Rodent dynamics as community processes. *Trends Ecol.*
536   *Evol.* **3**, 195-200 (1988).
537   49. D. Ehrich *et al.*, Documenting lemming population change in the Arctic: Can we
538   detect trends? *Ambio* **49**, 786-800 (2019).
539   50. M. Plummer (2003) JAGS: A program for analysis of Bayesian graphical models
540   using Gibbs sampling. in *Proceedings of the 3rd International Workshop on*
541   *Distributed Statistical Computing* (Vienna, Austria).
542   51. A. Gelman, B. Goodrich, J. Gabry, A. Vehtari, Rsquared for Bayesian regression
543   models. *Am. Stat.* **73**, 307-309 (2019).

544 52. A. Stien *et al.*, Congruent responses to weather variability in high arctic herbivores. *Biol. Lett.* **8**, 1002-1005 (2012).

546 53. R. Choquet, L. Rouan, R. Pradel, "Program E-Surge: a software application for fitting multievent models" in Modeling Demographic Processes In Marked Populations, D. L. Thomson, E. G. Cooch, M. J. Conroy, Eds. (Springer US, Boston, MA, 2009), 10.1007/978-0-387-78151-8_39, pp. 845-865.

550 54. D. R. Anderson, K. P. Burnham, G. C. White, AIC model selection in overdispersed capture-recapture data. *Ecology* **75**, 1780-1793 (1994).

552 55. V. Grosbois *et al.*, Assessing the impact of climate variation on survival in vertebrate populations. *Biol. Rev.* **83**, 357-399 (2008).

554 56. L. Oksanen, Exploitation ecosystems in seasonal environments. *Oikos* **57**, 14-24 (1990).

556 57. P. Turchin, G. O. Batzli, Availability of food and the population dynamics of arvicoline rodents. *Ecology* **82**, 1521-1534 (2001).

558 58. M. Kot, W. M. Schaffer, The effects of seasonality on discrete models of population growth. *Theor. Popul. Biol.* **26**, 340-360 (1984).

560 59. E. R. White, A. Hastings, Seasonality in ecology: progress and prospects in theory. *Ecol. Complex.* **44**, 100867 (2020).

562 60. O. N. Bjornstad, W. Falck, N. C. Stenseth, Geographic gradient in small rodent density-fluctuations - a statistical modeling approach. *Proc. R. Soc. B-Biol. Sci.* **262**, 127-133 (1995).

565 61. G. Gauthier, D. Berteaux, C. J. Krebs, D. Reid, Arctic lemmings are not simply food limited - a comment on Oksanen et al. *Evol. Ecol. Res.* **11**, 483-484 (2009).

567 62. P. Turchin, L. Oksanen, P. Ekerholm, T. Oksanen, H. Henttonen, Are lemmings prey or predators? *Nature* **405**, 562-565 (2000).

569 63. T. Klemola, M. Koivula, E. Korpimäki, K. Norrdahl, Experimental tests of predation and food hypotheses for population cycles of voles. *Proc. R. Soc. B-Biol. Sci.* **267**, 351-356 (2000).

572 64. R. Boonstra, C. J. Krebs, N. C. Stenseth, Population cycles in small mammals: the problem of explaining the low phase. *Ecology* **79**, 1479-1488 (1998).

574 65. R. A. Ims, Male spacing systems in microtine rodents. *Am. Nat.* **130**, 475-484 (1987).

576 66. O. Gilg, I. Hanski, B. Sittler, Cyclic dynamics in a simple vertebrate predator-prey community. *Science* **302**, 866-868 (2003).

578 67. I. Hanski, P. Turchin, E. Korpimaki, H. Henttonen, Population oscillations of boreal rodents: regulation by mustelid predators leads to chaos. *Nature* **364**, 232-235 (1993).

581 68. J. Aars, R. A. Ims, Intrinsic and climatic determinants of population demography: the winter dynamics of tundra voles. *Ecology* **83**, 3449-3456 (2002).

583 69. F. Domine *et al.*, Snow physical properties may be a significant determinant of lemming population dynamics in the high Arctic. *Arctic Sci.* **4**, 813-826 (2018).

585 70. L. Korslund, H. Steen, Small rodent winter survival: snow conditions limit access to food resources. *J. Anim. Ecol.* **75**, 156-166 (2006).

587 71. K. L. Kausrud *et al.*, Linking climate change to lemming cycles. *Nature* **456**, 93-U93 (2008).

590 **Tables**

591

592 Table 1. Parameter estimates for the best models for monthly population growth of
593 Eastern European voles (equations 1-5) over winter and in the summer period and
594 estimates of the Bayesian R^2 for the models. No rain-on-snow (ROS) effect was included
595 in the model for summer population growth, giving no estimate of β_{ROS}.

Parameter	Winter		Summer	
	mean	95 % C. I.	mean	95 % C. I.
β_0	0.23	(0.14, 0.33)	0.64	(0.44, 0.83)
β_D	-0.0040	(-0.0058, -0.0024)	-0.0051	(-0.0095, -0.0006)
β_{ROS}	-0.0043	(-0.0074, -0.0014)	-	-
σ_r^2	0.005	(0.001, 0.020)	0.020	(0.005, 0.058)
Bayesian R^2	0.92	(0.73, 0.98)	0.40	(0.02, 0.76)

596 β_0 = intercept; β_D = coefficient for density at time t; β_{ROS} = coefficient for effect of ROS;
597 σ_r^2 = process error variance.

Figures

Fig. 1. Picture of the Core and Ridge areas for live-trapping East European voles near
Grumantbyen on Svalbard (**a**) and time series of vole densities (**b**) estimated in August in
the Core area (gray shape, lines points, years 1990-1996 and 2002-2006) and the Ridge
area (black shape, lines and points, years 1991-2007). Error bars represent 95%
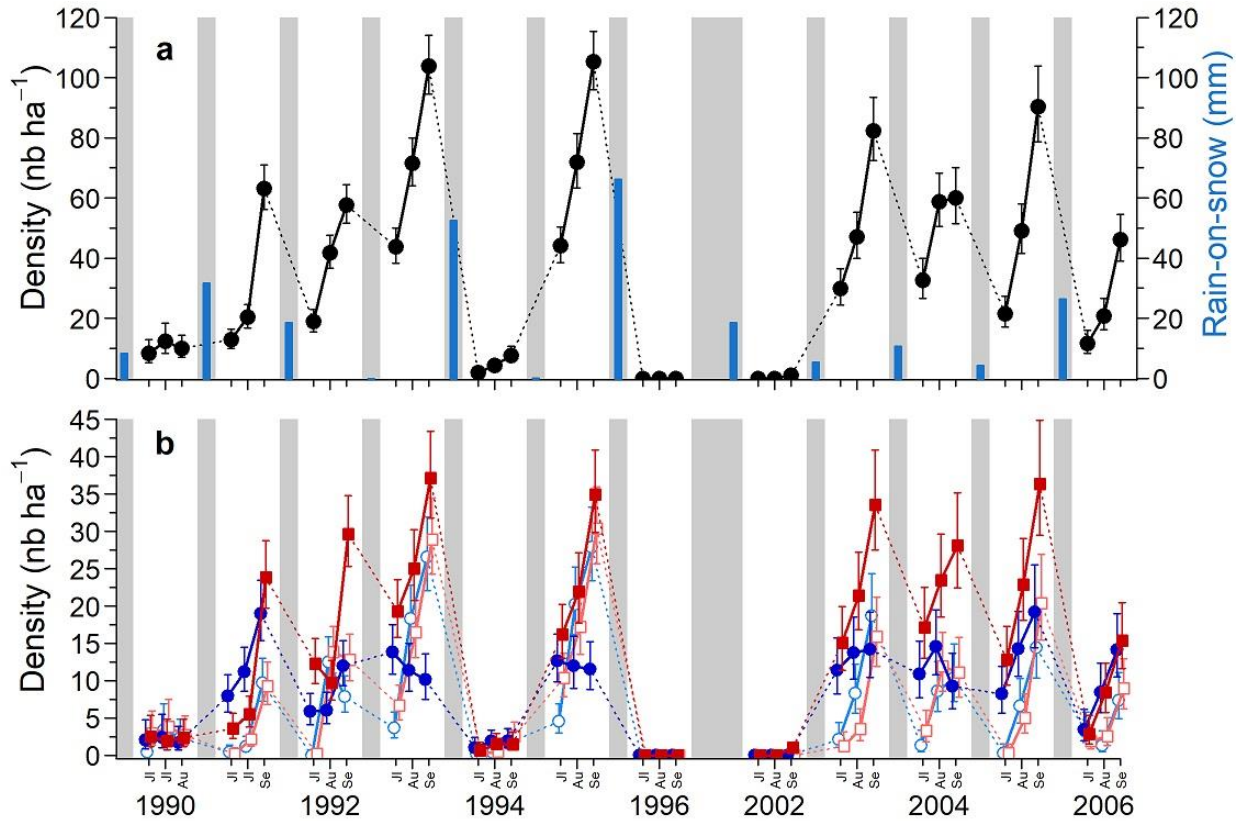confidence intervals.

606
607 Fig. 2. Population density of the East European vole in the Core area near the Grumant
608 area in Svalbard (lines and points) and precipitation as rain-on-snow during the previous
609 winter (blue bars in **a** only). The total population densities are shown in **a**. In **b**, adult
610 males (solid blue circles and lines), adult females (solid red squares and lines), subadult
611 males (open pale blue circles and lines), and subadult females (open pale red squares and
612 lines) are shown. Densities were obtained using spatially-explicit capture-recapture
613 models with the Huggins parameterisation. Dotted lines indicate change in population
614 size during winter. The thin grey bands indicate winter when trapping was not conducted.
615 The wide grey band between 1996 and 2002 indicate no trapping during that period.
616 Error bars represent 95% confidence intervals. Notice the difference in scale between **a**
617 and **b**. In 1990, trapping periods were in early July, late July, and mid-August. In 1991,
618 trapping periods were early July, late July, and mid-September, whereas for all other
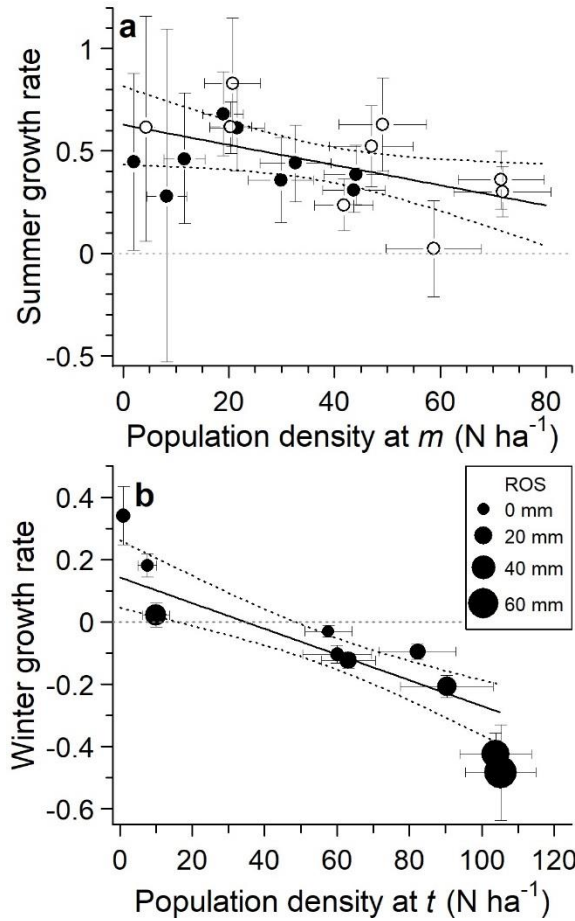619 years trapping was done in the first part of each month.
620
621

Fig. 3. Estimated monthly population growth rates (r) in summer in relation to population density in month *m* (**a**) and monthly winter population growth rate in relation with population density in year *t* measured in September (**b**) of East European voles. In **a**, filled points represent the early summer period (July-August) and open points the late summer period (August-September) each year. In **b**, the points represent average monthly growth over the period September-July and point size reflect the amount of rain-on-snow (ROS, mm) that fell during the winter. Error bars represent 95% confidence and credibility intervals along respectively the x and y - axis. Parameter estimates for the regression lines (with 95% C.I.) are given in Table 1. Horizontal dotted gray line mark r = 0, no change in population size.
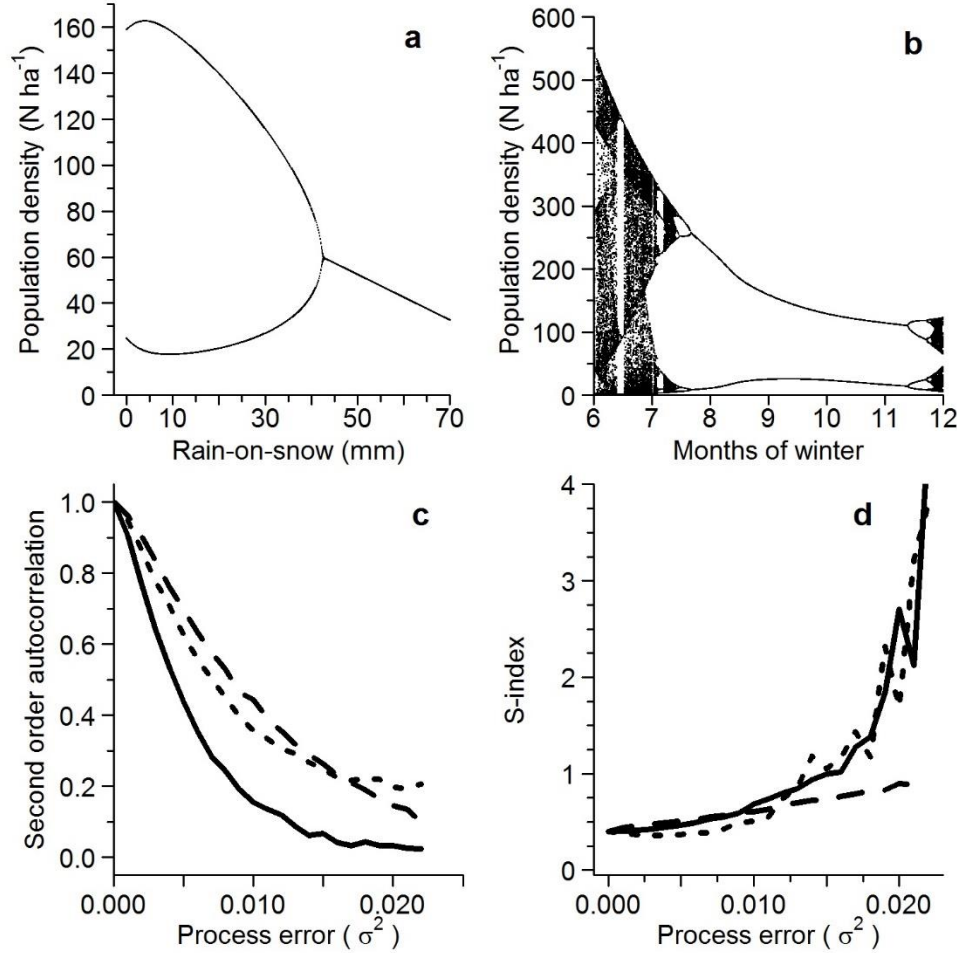
Fig. 4. Simulated population dynamics in the East European vole in Svalbard. (**a**) Bifurcation diagram for autumn densities for increasing fixed amounts of rain-on-snow (ROS) every winter using the population model with no process error ($r_{w,t} = \beta_{w,0} + \beta_{w,X} * X_{w,t} + \beta_{w,ROS} * ROS_t$, parameter estimates in Table 1 but $\sigma_{i,r}^2$ set to zero). (**b**) Bifurcation diagram for the effect of changing the length of the winter season (Δt_w) on autumn densities in the baseline population model with zero ROS and process error (ROS = 0, σ_r^2 = 0). (**c**) Estimates of the second order autocorrelation and (**d**) the amplitude of fluctuations (s-index) in autumn densities in the baseline population model for increasing values of process error variance (σ_r^2) and ROS = 0. In **c** and **d**, the long dashed line represents a model where process error only affects the summer population growth, the short dashed line a model where process error only affects the winter population growth, and the solid line represents a model where process error affects equally winter and summer population growth. Estimates of process error variance in models without a ROS effects were $\bar{\sigma}_{w,r}^2$ = 0.014 and $\bar{\sigma}_{s,r}^2$ = 0.020 for winter and summer, respectively. Estimated second order autocorrelation in the Ridge area in August was 0.02, while the s-index was 0.57.
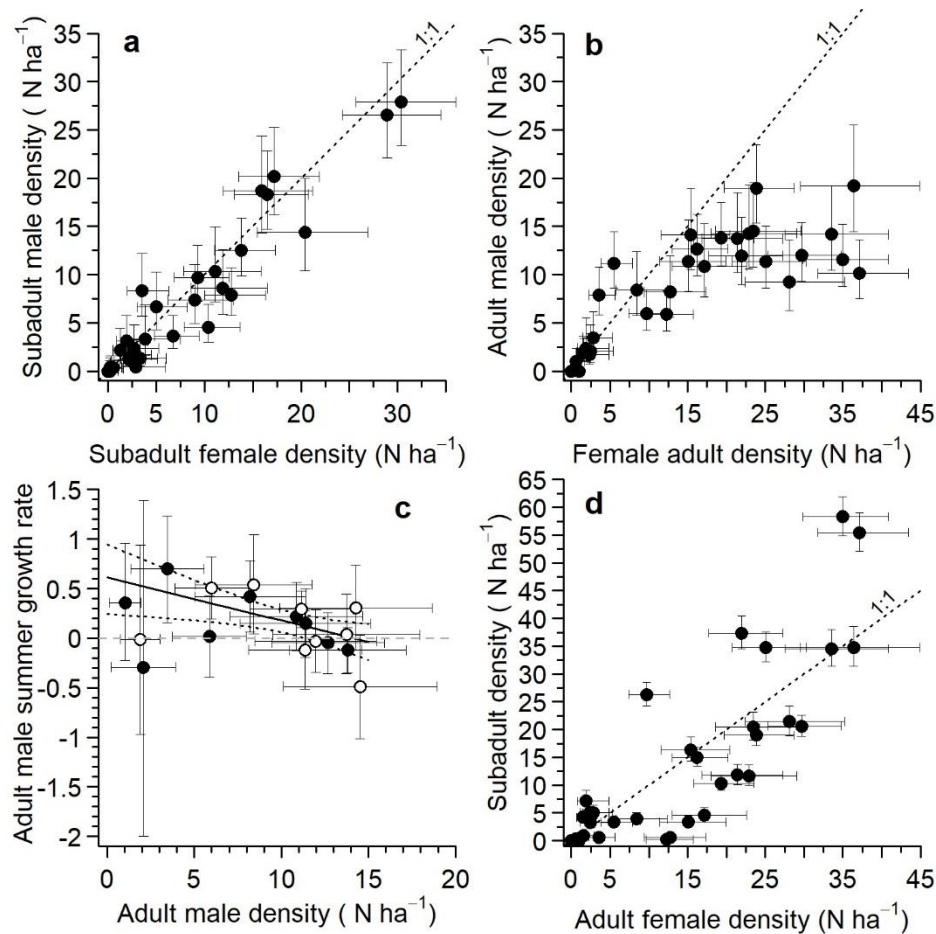
Fig. 5. Demographic structure and density dependence based on sex and body size (i.e. sub-adult vs. adults) of East European voles. Sex ratio displayed as **a** the density of sub-adult males plotted against the density of sub-adult females and as **b** density of adult males plotted against the density of adult females. In **c**, density dependence in adult males in summer displayed as estimated monthly population growth rate (from time *t* to *t*+1) in adult males plotted against the density of adult males at time t. Estimates from the early (July-August) and late part of the summer (August – September) are given by closed and open circles, respectively. The full line is the regression line estimated using equations (1-5; β_D = -0.043, CI=[-0.073, -0.009]). Black dotted lines are the 95% C.I. for the regression line and the grey dashed horizontal line represents zero population growth. In **d**, recruitment as measured by the density of sub-adults is plotted against the adult female population density. In **a**, **b** and **d**, the 1:1 dotted lines are drawn for visual reference. Bars gives the 95% confidence intervals of estimated densities (**a**-**d**) and population growth rates (**c**).

Supplementary material

669

670 **Methodological adjustments adopted to handling low and zero population densities**
671 **when estimating of population growth**
672 In September 2002 there were only 3 voles caught and the density was estimated to 1
673 vole per hectare. However, the mark-recapture analysis did not allow measurement error
674 to be estimated for this density estimate. To overcome this problem with a missing value
675 for the uncertainty associated with the density estimator in subsequent analyses we used
676 the empirical least square linear relationship between $\log(D_t)$ and $\log(\text{var}(D_t))$,
677 $\log(\text{var}(D_t))= -1.5253 - 0.9479 * \log(D_t))$, to estimate $\sigma_{D,t}^2$ for the last observation in
678 2002.
679   In June/July 1996, no vole was caught giving an estimate of zero density of voles.
680 No vole was caught in the Core area also in the subsequent trapping periods in 1996, as
681 well as the nearby Ridge area. The most reasonable explanation for the zero observations
682 in 1996 was therefore local extinction in the trapping area, and not that a zero due to
683 measurement error. The previous winter had the highest levels of ROS in the dataset and
684 the population density the previous autumn was also the highest observed, so the
685 handling of the zero observation in 1996 could affect estimates of the effect of density
686 dependence and ROS on winter population growth rates. In our estimation of population
687 growth we imputed a small number for the zero observation in June/July 1996. We
688 evaluated the consequence of different choices for the imputed value by fitting the model
689 (equations 1-3) with imputed values for the density in June/July 1996 in the range δ =
690 [0.1, 1], where 1 vole per hectare is the lowest positive estimate of the density of voles in
691 the study area. Changes in the imputed value mainly affected estimates of the effect of
692 ROS, with increasingly negative estimates of β_C with decreasing δ (point estimates
693 decreasing from -0.0042 to -0.0052). Estimates of β_X (density dependence) were robust to
694 the choice of δ (point estimate range = (-0.0041, -0.0042)). In the results we use δ = 1.
695 This value of δ gave similar parameter estimates to models fitted to data with the
696 observation from June/July 1996 excluded. However, it is noteworthy that more negative
697 effect sizes of ROS are also consistent with the data.

698

699 **Detailed results from the survival and maturation analyses**
700 The data supported a model for survival that included an additive effect of year, and an
701 interaction effect between trapping period, age, and sex (Table S1). Apparent survival
702 rates were highest for adult females (~75-85%/month), whereas sub-adult males had the
703 lowest apparent survival rates (~15-65%/month; Fig. S2). Adult females showed no
704 change in survival rates between the early (July-August) and late (August-September)
705 summer periods. For the other demographic groups of voles survival rates were lower in
706 late summer than early summer (Supplementary material, Fig. S1). This period effect in
707 the survival of males and juvenile females, as well as high survival estimates for the years
708 with very low densities (1990 and 1994), was consistent with density-dependent survival
709 density at t and survival between t and $t + 1$ (Fig. S2). The ANODEV confirmed that the
710 survival was negatively affected by density, but this effect was more pronounced in males
711 than females (β = -0.025, 95% CI=[-0.036, -0.013]; Table S2, Fig. S2).
712   Maturation rates varied between years and with an interaction effect between
713 trapping period and sex (Table S1, Fig. S1). We found no significant relationship with

714 density at time *t* based on the most parsimonious, non-temporal model ($\beta = 0.006$, 95%
715 CI: [-0.011: 0.023]; Table S2; Fig. S3). Both sexes had high maturation rates for the July-
716 August period, with males having a 100% maturation probability in all years in this first
717 part of the summer (Fig. S1). Maturation rates were substantially lower in the latter part
718 of the summer (August-September), and males tended to have lower maturation rates
719 than females in this period (Fig. S1).
720
721

722 Table S1. Ranking of models to test for the effects of time and density on survival (φ) and
723 transition (ψ; maturation) rates of East European voles. The formulae of each model (i) is
724 shown along with its number of parameters (K), ranking parameter $\Delta QAICc_i$, and model
725 weight (w_i). We modelled detection the same way for all models with additive effects of
726 period (t), year, age, and sex. The models that are shown represent those with the highest
727 statistical support ($\Delta QAICc_i < 2$) for the three hypotheses being tested. Time-dependent
728 models shown are those with a $\Delta QAICc_i < 4$ and the one ranked right after. For the
729 density dependence analyses, we present the models with the highest support without
730 temporal effects and $\Delta QAICc_i$ are calculated based on the top time-dependent model.

	Model			
Type	φ	ψ	K_i	$\Delta QAICc_i$
Time-dependent	year+t.f.sex	year+t.sex	44	0.00
	year+t.sex+f.sex	year+t.sex	42	4.05
Density-dependent survival	D.sex+f.sex	year+t.sex	33	9.87
	D.f.sex+f.sex	year+t.sex	35	10.86
	D+sex	year+t.sex	32	11.22
Density-dependent maturation	year+t.f.sex	D+sex	34	58.54
	year+t.f.sex	D.sex+sex	35	59.08

731 Note: covariates on detection probabilities were the same for all models and included
732 additive effects of year, primary period, state (subadults, adults), and sex.
733 t = primary period (July-August, August-September); D = relative density (low,
734 intermediate, high); f = state; + = additive effect; . = interactive effect.
735

736

737   Table S2. Analysis of deviance (ANODEV) for models without temporal effects to assess
738   density dependence in survival (φ) and maturation (ψ) of East European voles.

Model				
Response variable	φ	ψ	F-value	p-value
Survival	D.sex+f.sex	year+t.sex	3.299	0.043
Maturation	year+t.f.sex	D+sex	6.109	0.018

739   Note: Model comparisons for the ANODEV were based on the full time-dependent
740   model ($\varphi \sim$ year+t.f.sex, $\psi \sim$ year+t.sex, $p \sim$ year+t+f+sex; $K = 44$) and the simplified
741   model without time or density as a covariate on survival ($\varphi \sim$ f.sex, $\psi \sim$ year+t.sex, $p \sim$
742   year+t+f+sex; $K = 31$) or maturation ($\varphi \sim$ year+t.f.sex, $\psi \sim$ sex, $p \sim$ year+t+f+sex; $K =$
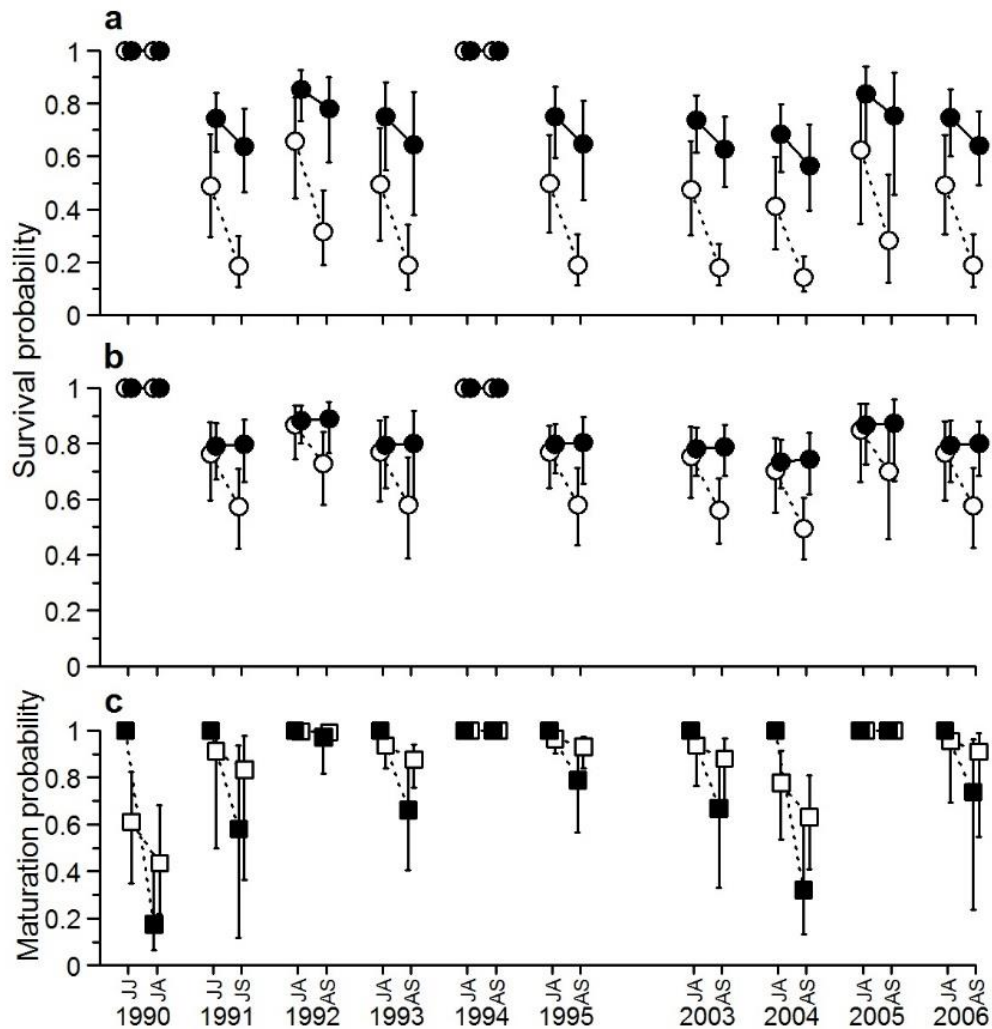743   33).

744

745
746 Fig. S1. Summer survival estimates of adult (black circles) and sub-adult (white circles)
747 male (**a**) and female (**b**) East European voles and maturation probabilities (**c**) of sub-adult
748 males (white squares) and females (black squares) throughout the years of sampling. Data
749 points are slightly displaced on the x-axis to make confidence intervals more visible. The
750 gap between 1995 and 2003 indicate no data available for summers of 1996-2002 due to
751 sample size being too low or trapping occurred only in August. Error bars are 95%
752 confidence intervals. JJ: early July to late July; JA: late July (1990 only) or mid-July (all
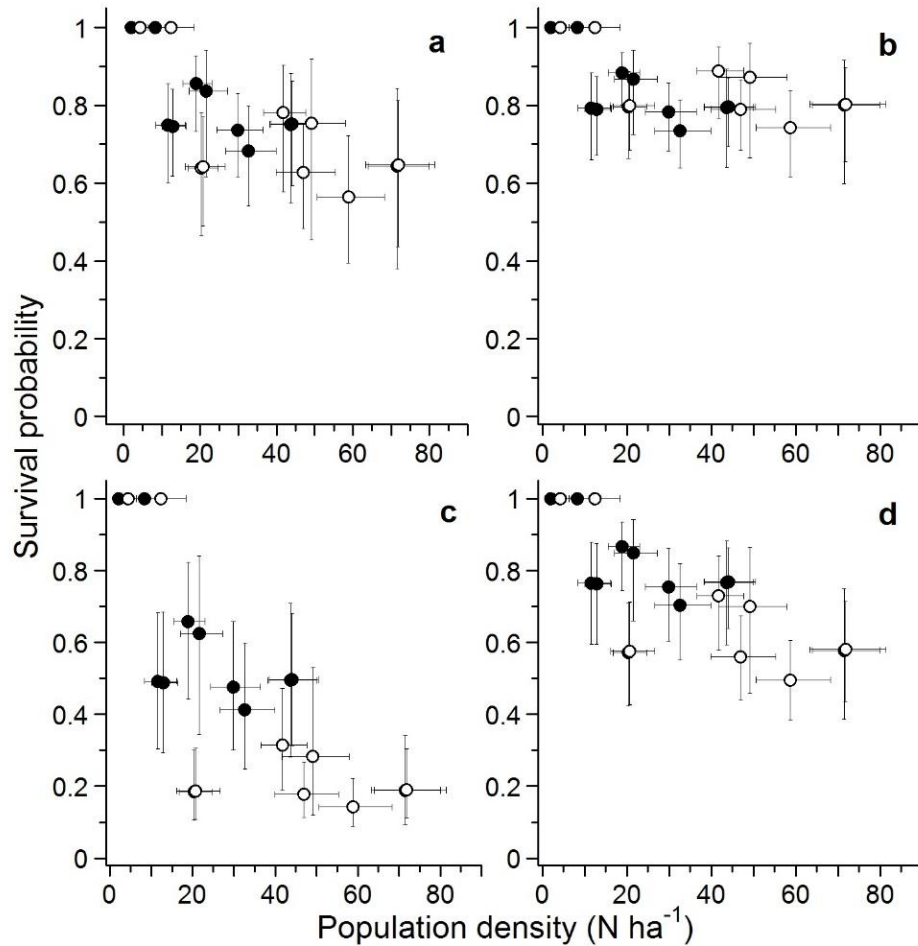753 other years) to mid-August; JS: late July to mid-September; AS: mid-August to mid-
754 September.
755

756
757 Fig. S2. Estimates of survival rates in East European voles between *t* and *t*+1 of adult
758 males (**a**), adult females (**b**), subadult males (**c**), and subadult females (**d**) in relation with
759 population density at *t* from the most parsimonious model (Table S1, time-dependent
760 model $\varphi = f$(year+t.f.sex)). Filled points represent the period of July-August and open
761 points the August-September period, error bars represent 95% confidence intervals.
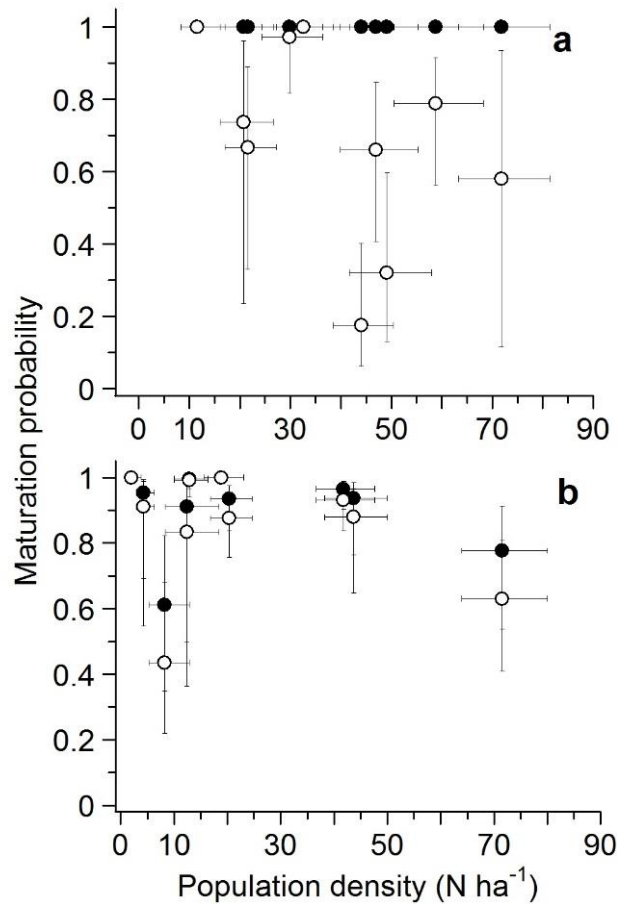762
763

764
765 Fig. S3. Estimates of maturation rates in East European voles for subadult males (**a**) and
766 females (**b**) from a model with an additive effect of year, and an interaction effect
767 between live-trapping period and sex ($\psi = f(year+t.sex)$, Table 1). Filled points represent
768 the period of July-August and open points the August-September period, error bars
769 represent 95% confidence intervals. Correlation coefficients are given using all the data
770 points (r.all) and excluding the estimates of $\psi = 1$ (r.sub).
771
772